

Design and Fabrication of gas sensor and its applications as IoT Devices

Submitted in partial fulfillment of the requirements

of the degree of

Bachelor of Technology

by

Ms.Sneha Choudhary(20115068)

Nisha Kumari(20115074)

Tejasvi Arya(20115155)

Tushar N Gupta(20115157)

Supervisor(s)

Prof. P.Sumathi



Department of Electrical Engineering
Indian Institute of Technology Roorkee

2023-24

Declaration

I hereby declare that the work which is presented here, entitled Design and Fabrication of Gas Sensor and its application as IoT Devices, submitted in partial fulfillment of the requirements for the award of the Degree of Bachelor of Technology in the Department of Electrical Engineering, Indian Institute of Technology Roorkee. I also declare that I have been doing my work from Month Year under the supervision and guidance of Prof. P. Sumathi, Department of Electrical Engineering, Indian Institute of Technology Roorkee. The matter presented in this dissertation report has not been submitted by me for award of any other degree of institute or any other institutes.

Date: 23/04/2024

Signature:

Name: Ms.Sneha Choudhary, Nisha Kumari, Tejasvi Arya, Tushar N Gupta

Enrolment Number: 20115068,20115074,20115155,20115157

Certificate

This is to certify that the above statement made by the candidate is true to best of my knowledge and belief.

Signature

Prof. P. Sumathi

Designation

Department of Electrical Engineering

Indian Institute of Technology Roorkee

Acknowledgment

We would like to express our sincere gratitude to our project Supervisor, Prof. P. Sumathi for their contribution to our B.Tech Project titled “Design and Fabrication of gas sensor and its application as IoT Devices”. Your invaluable guidance and support played a crucial role in the progress of our project.

We also thank PhD research scholar Ms. Nikhila Patil for providing guidance and suggestions. Their suggestions and guidance were beneficial in enhancing our knowledge about the topic.

We greatly appreciate the time and effort you put into reviewing and providing feedback on our project at various stages. Your expertise and knowledge in the field have been instrumental in shaping our ideas and understanding of the subject matter. Your encouragement and motivation throughout the project have been a source of inspiration for us.

We would also like to thank you for sharing your valuable resources, references, and contacts which proved to be invaluable assets in the progress of our project.

Once again, thank you for your support and guidance throughout the project. It has been an honor to work with you, and we hope to collaborate on future projects.

Sincerely,
Ms.Sneha Choudhary
Nisha Kumari
Tejasvi Arya
Tushar N Gupta

Abstract

A gas sensor based on micro-electromechanical systems (MEMS) can detect and measure the concentration of gases in the surrounding atmosphere. This report demonstrates the design and simulation of different Platinum micro-heaters for sensor applications. These microheaters have been precisely engineered for low thermal mass, minimal power consumption, and excellent temperature uniformity[1]. The shape of the microheater was optimized by running simulations of many conceivable patterns in COMSOL Multiphysics 6.0. We showed four distinct microheater patterns: single meander, spiral meander, spiral, and double meander as well as their accompanying electro-thermal simulated temperature profiles.

Table of Contents

Abstract.....	4
List of Figures	6
1 Introduction	7
2 Micro heater	9
2.1 Meander geometry	10
2.2 Spiral geometry	11
2.3 Spiral-Meander geometry	
2.4 Double Meander geometry	12
3 Simulation environment	14
4 Materials used for microheaters	15
5 Heater simulations	16
6 Why use platinum?	19
7 Inter-digital electrodes (IDEs)	20
8 Sensing layer	21
9 Velocity profile of Gas Chamber	22
10 IOT implementation of gas sensor	24
11 Fabricated gas sensor	27
12 Conclusions	31
References	32

List of Figures

- Fig1. Micro-heater-based gas sensor design
- Fig2. Micro-heater testing
- Fig3. Geometry of Meander Structure
- Fig4. Graph Simulation of Meander Structure
- Fig5. Geometry of Spiral Structure
- Fig6. Graph simulation of Spiral Structure
- Fig7. Geometry of Spiral-Meander Structure
- Fig8. Graph Simulation of Spiral-Meander Structure
- Fig9. Geometry of Double Meander Structure
- Fig10. Graph Simulation of Double Meander Structure
- Fig11. Environment for simulation
- Fig12. Velocity and concentration profile of NO₂ gas flow in simulation environment.
- Fig13. Velocity and concentration profile of NO₂ gas with heater engaged.
- Fig14. Meander Geometry used in fabricated sensor
- Fig15. Voltage-Current data for NO₂ gas
- Fig16. I vs V curve of fabricated gas sensor

Chapter 1

Introduction

Gas sensors are essential parts of many household and commercial applications because they make it possible to identify and keep track of the many gases present in the surrounding air. By offering real-time data on gas concentrations, these sensors optimize several processes. A multidisciplinary approach is used in the design and construction of gas sensors, combining concepts from electrical engineering, chemistry, and materials science.

For precise and dependable gas detection, careful consideration of the architecture of the sensor, the qualities of the sensing material, and the integration of auxiliary components are necessary for efficient gas sensor design. Research and development in this field continue due to the constant demand for better sensor performance, including higher sensitivity, selectivity, and stability.

MEMS gas sensors can detect a wide range of gas components in the atmosphere, including CO₂, CO, NO₂, and SO₂. Many gas-sensing materials, like semiconducting metal oxides, require high temperatures to work properly. Metal oxide gas sensors use surface adsorption properties to measure changes in resistance when gas concentrations change. Since the microheater's temperature affects the gas sensor's sensitivity and response time, it is imperative to get the heater up to the necessary working temperature.

MEMS gas sensors are used in various applications, including medical diagnostics, industrial production, security testing, and environmental monitoring. Thus, we studied various micro-heater geometries to determine their potential to supply the required warmth uniformly and efficiently[2].

This thorough overview explores the fundamentals of creating and manufacturing gas sensors, highlighting important factors to consider while choosing materials, designing sensor architectures, fabricating techniques, and testing procedures. The complex design and fabrication process can be understood to produce highly efficient gas sensors that satisfy the demanding requirements of contemporary industrial and environmental monitoring applications.

Gas sensor design:

The overall structure for the gas sensor which includes supporting layer, heater, insulating layer, IDEs and sensing layer is shown below.

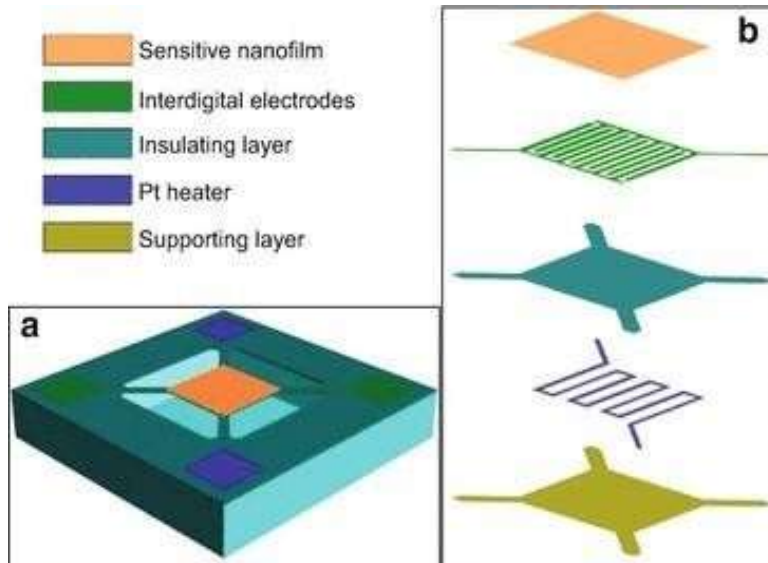


Fig1. Micro-heater based gas sensor design[9]

Chapter 2

Micro-Heater

A microheater is a small heating device that is used to accurately and locally control temperature in a variety of applications. These small heating components are often fabricated using microfabrication techniques, which allows for exact dimensions and high control. Applications for micro warmers are many and include sensors, electronics, medicinal devices, and microfluidics. They precisely regulate the temperature while heating particular components, substances, or amounts. As technology advances, microheaters find more and more applications in science, electronics, and medicine where precise and small-scale heating is essential. The geometry of the micro heater is selected based on the particular application needs and design limitations. Thin-film micro heaters are frequently made from materials including nichrome (NiCr), platinum (Pt), and gold (Au). These materials are appropriate for producing and dispersing heat in micro-scale devices because of their high electrical resistivity and thermal stability [3]-[6]. We are using the metals Platinum, Palladium, Silver, Gold as material for micro-heater whose properties are shown below by the COMSOL software.

Heater dimensions: 3cm x 3cm

The following are some common micro heater geometries:

2.1 Meander Geometry

Micro heaters often use the meander geometry because it can increase heat dissipation by making the most surface area possible in a small space. Effective heat distribution and consistent temperature profiles are made possible by the continuous serpentine or zigzag pattern of meandershaped micro heaters.

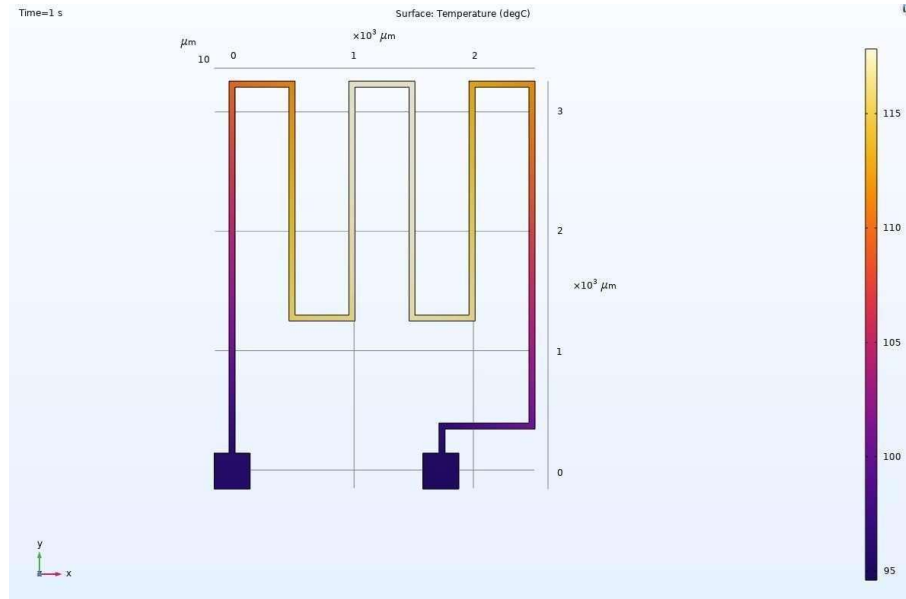


Fig3. Geometry of meander structure

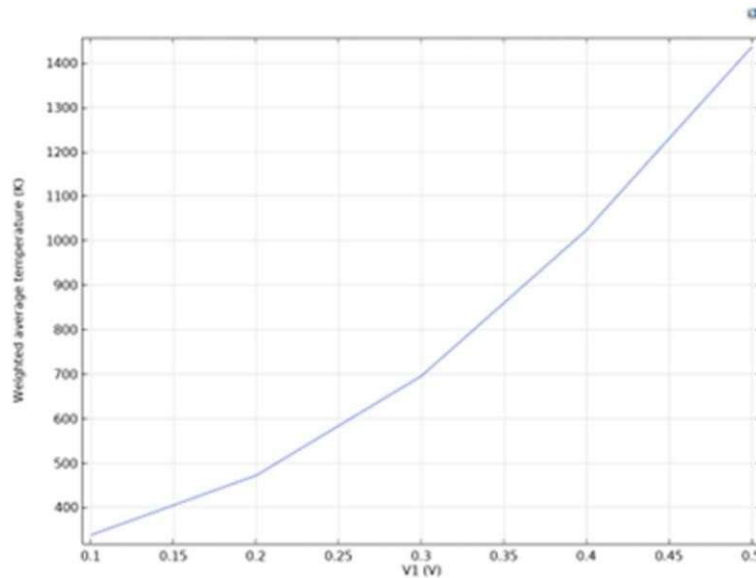


Fig4. Graph simulation of meander structure

2.2 Spiral Geometry

A shape that continuously widens (or narrows) around a central point or axis is referred to as having spiral geometry. The spiral geometry in the context of micro heaters refers to a spiral patterned heating element that is usually made by microfabrication methods. This shape makes it possible to generate and distribute heat in a small area efficiently.

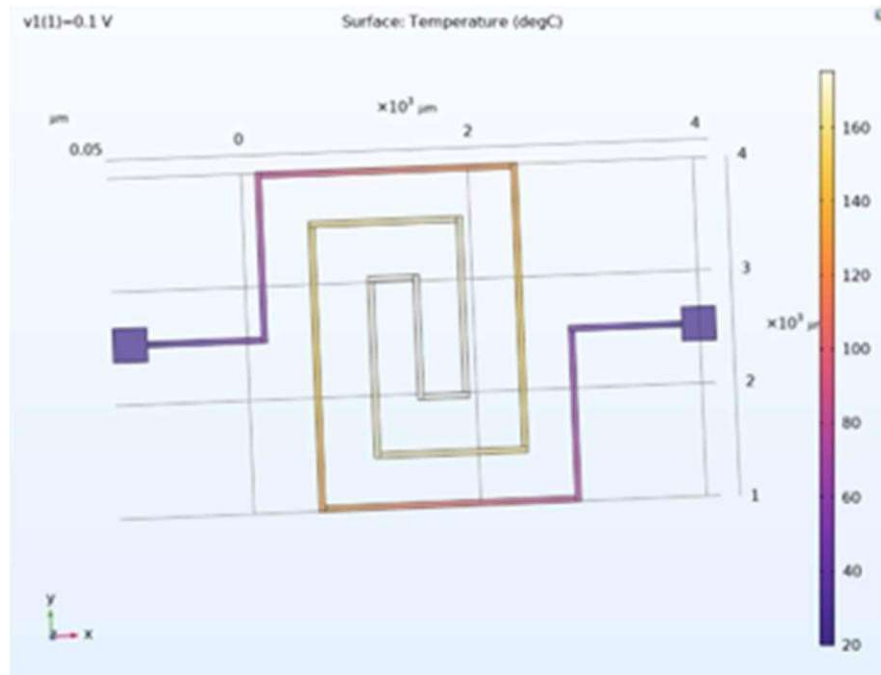


Fig5. Geometry of spiral structure

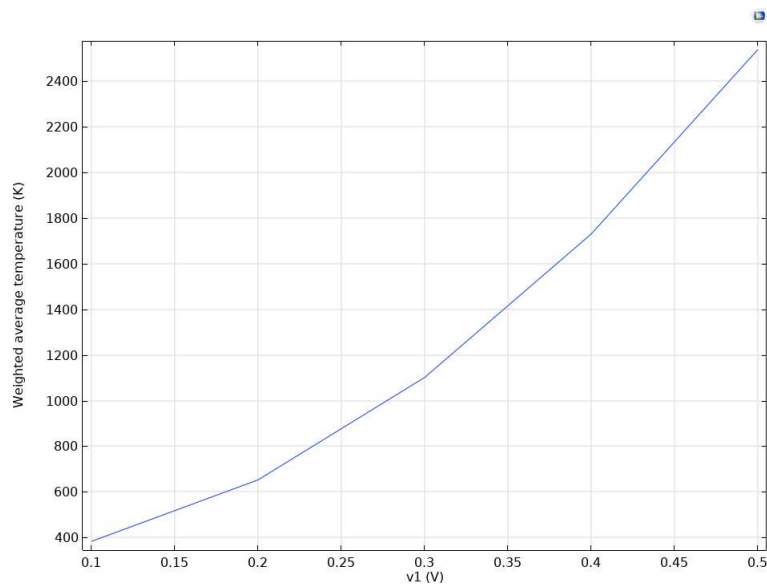


Fig6. Graph simulation of Spiral structure

2.3 Spiral-Meander Geometry

The spiral meander geometry is a complex yet extremely effective pattern for micro heaters that includes aspects of the spiral and meander geometries. This pattern combines elements of the spiral and meander designs; it frequently alternates between the two patterns or integrates them in a way that enhances each other along the heater's length. Combining these two geometries enables more accurate temperature control, better surface area use, and better heat distribution in micro-scale devices.

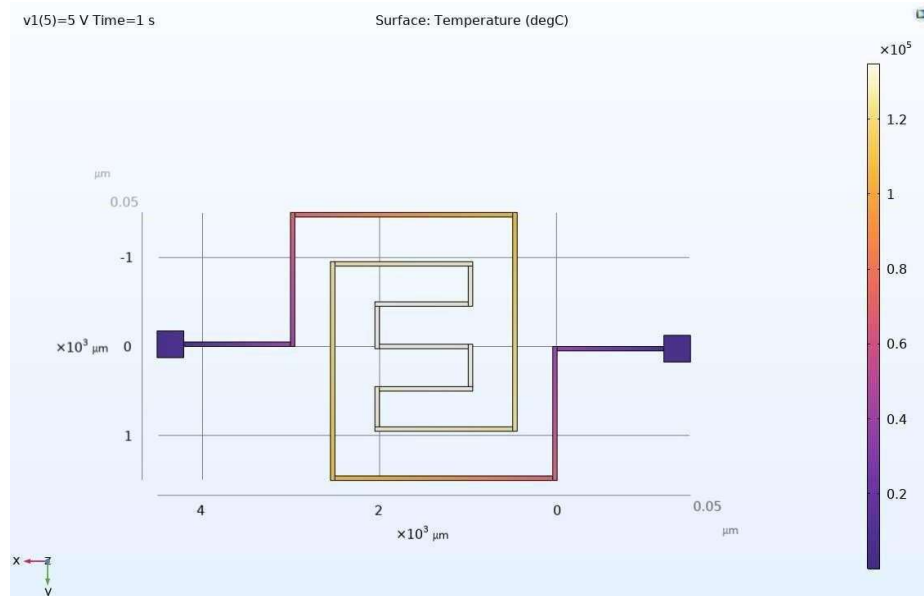


fig7. Geometry of Spiral-Meander

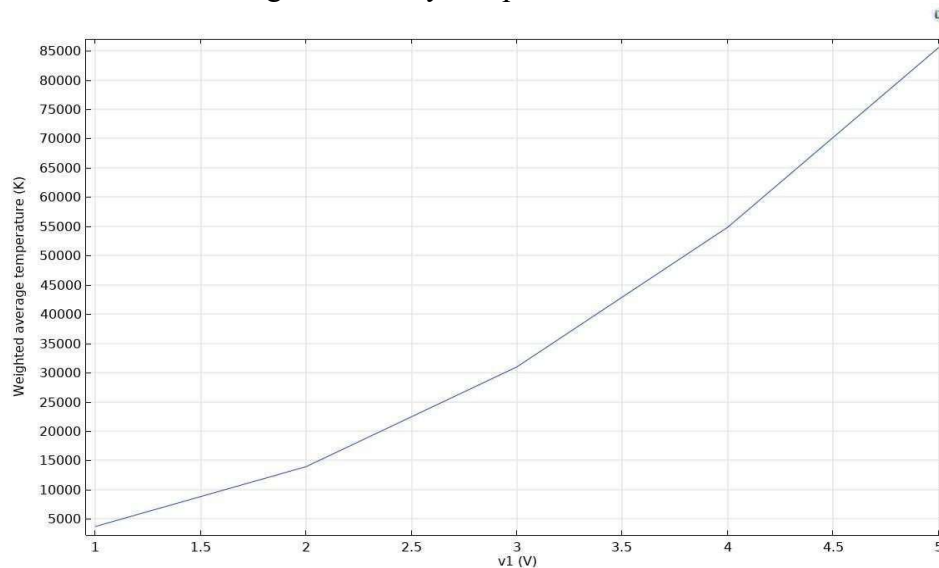


Fig8. Graph Simulation of Spiral-Meander

2.4 Double Meander Geometry

Double meander geometry is used in micro heaters to improve temperature uniformity, increase heating efficiency, and provide fine control over the heating process. In many microscale applications, such as chemical sensors, biomedical devices, and microfluidics, a more uniform dispersion of heat across the target region is made possible by this design.

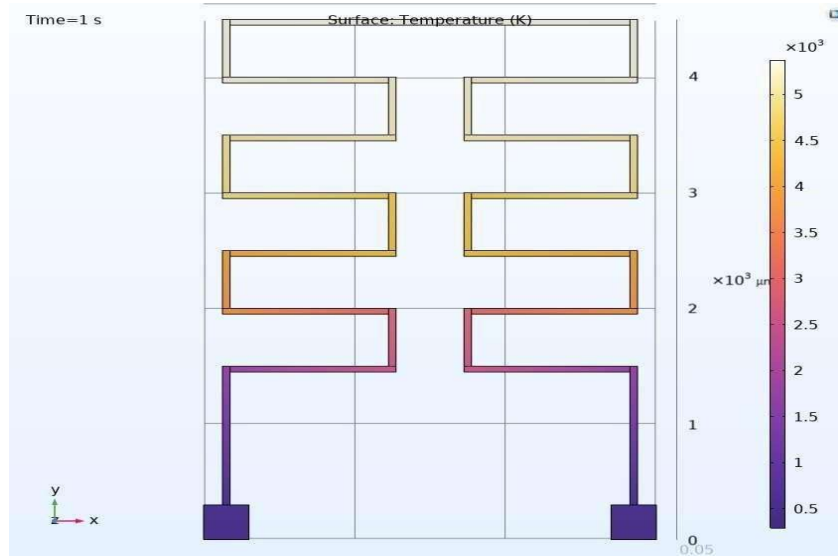


fig9. Geometry of Double Meander

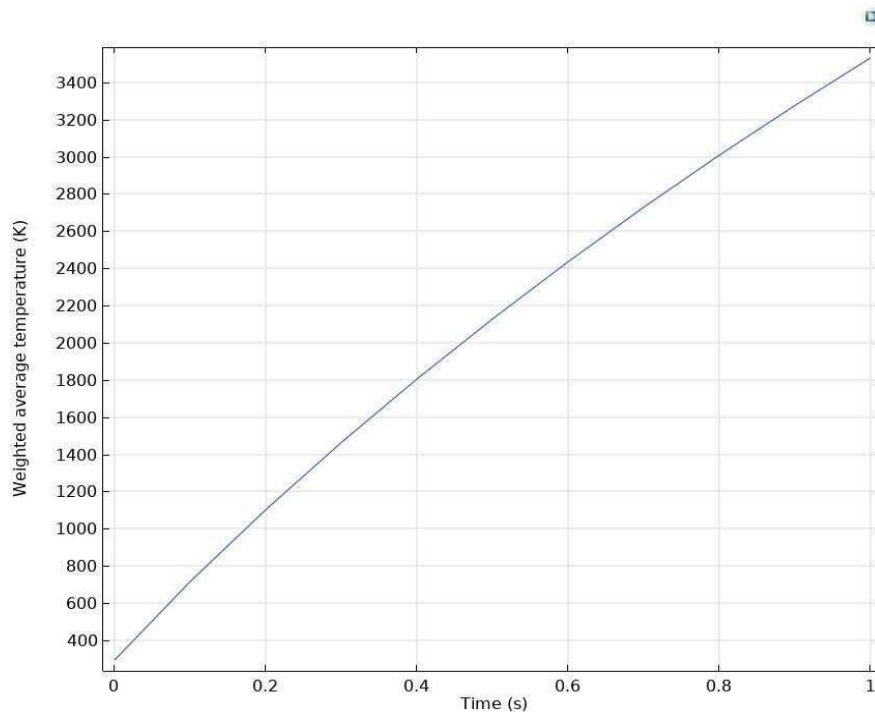


fig10. Graph Simulation of Double Meander

Chapter 3

Simulation Environment

The following image depicts the simulation environment built in COMSOL 6.1 software. Here, the microheater is placed on a silicon pad that will support the structure of the sensor. The sensor is then placed at the base of the cylinder. The cylinder/chamber has one inlet at the top and two small outlets at the bottom when helps in laminar flow the carrier air that carries the concentrated gas to be detected. The two outlets are equidistant from the centre to ensure symmetric flow of the air towards the sensor.

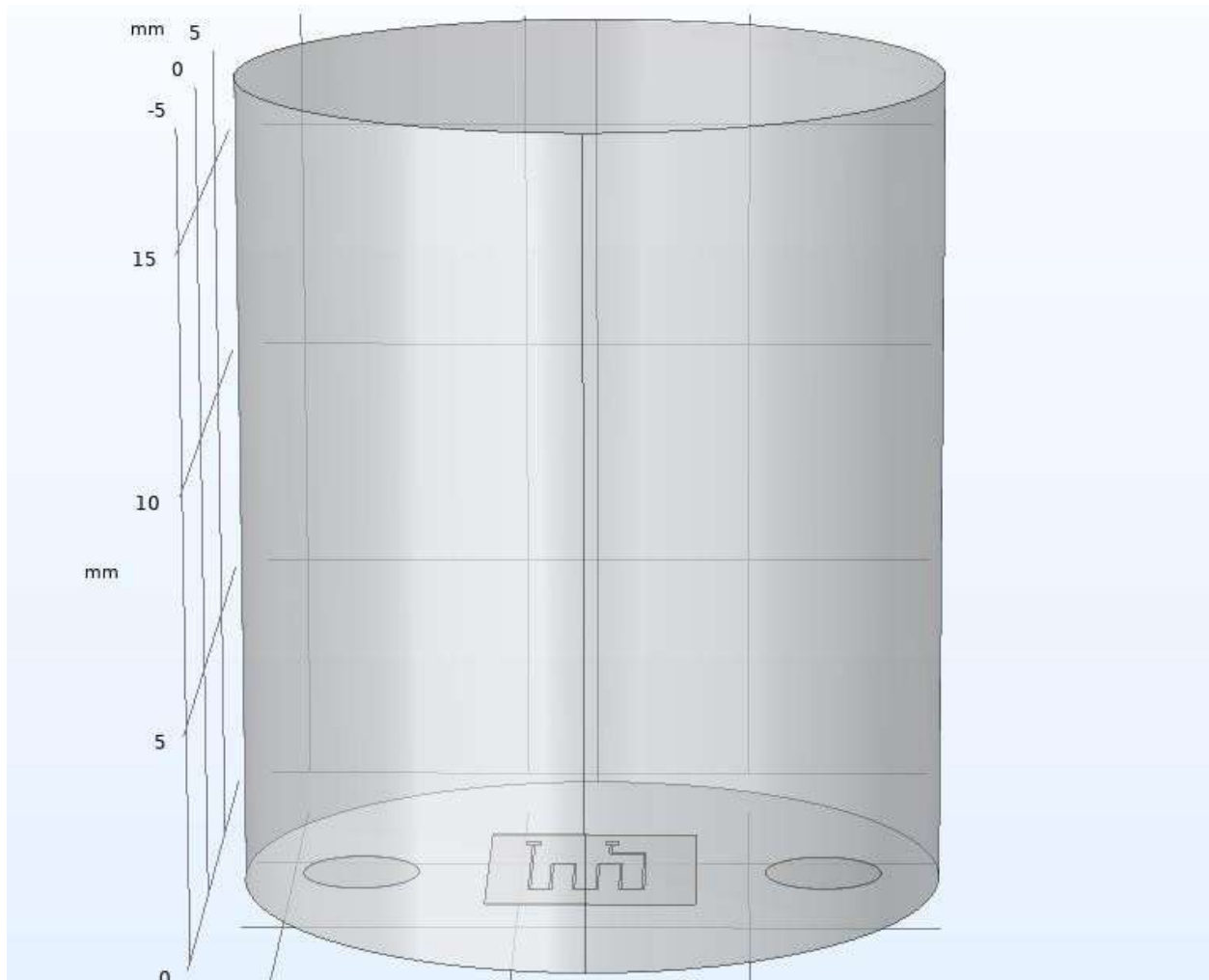


fig11. Environment for simulation

Chapter 4

Materials used for micro-heater

For the design of micro-heaters, we have used four materials. i.e., Platinum (Pt), Gold (Au), Palladium (Pd), Silver (Ag).

When constructing microheaters for MEMS gas sensors, materials like platinum (Pt), gold (Au), palladium (Pd), and silver (Ag) are often selected because of their many beneficial qualities. Due to their high electrical conductivity, these metals can effectively convert electrical energy into heat, which is necessary for microheaters to produce the necessary thermal output. Furthermore, they demonstrate strong chemical stability, which guarantees the sensor's durability and dependability even under demanding working circumstances or in the presence of reactive gases. They don't distort at the high temperatures required for gas sensing applications because of their comparatively high melting points. They may not have as high a thermal conductivity as some other materials, but they are still capable of effectively distributing and transferring heat throughout the microheater structure. Furthermore, Pt, Au, Pd, and Ag may be integrated into MEMS devices since they are compatible with semiconductor production techniques. For biomedical applications, their biocompatibility is favourable, especially in the case of gold and platinum. Additionally, these metals provide corrosion resistance, which is essential for preserving the stability and effectiveness of the sensor over time. Moreover, its low temperature coefficient of resistance (TCR) guarantees consistent and reliable heating properties in microheaters, enhancing the MEMS gas sensor's overall performance. The physical properties of the materials are mentioned below:

»	Property	Variable	Value	Unit
<input checked="" type="checkbox"/>	Electrical conductivity	sigma...	10.0e6[S...	S/m
<input checked="" type="checkbox"/>	Heat capacity at constant pres...	Cp	244[J/(k...	J/(kg·K)
<input checked="" type="checkbox"/>	Density	rho	12020[k...	kg/m³
<input checked="" type="checkbox"/>	Thermal conductivity	k_iso ;...	71.8[W/(...	W/(m·K)
<input checked="" type="checkbox"/>	Relative permittivity	epsilo...	1.00692	1
<input checked="" type="checkbox"/>	Coefficient of thermal expansion	alpha_...	11.8e-6[...	1/K
	Young's modulus	E	73e9[Pa]	Pa
	Poisson's ratio	nu	0.44	1

Palladium

»	Property	Variable	Value	Unit
<input checked="" type="checkbox"/>	Electrical conductivity	sigma_...	8.9e6[S/m]	S/m
<input checked="" type="checkbox"/>	Heat capacity at constant pressure	Cp	133[J/(kg...	J/(kg·K)
<input checked="" type="checkbox"/>	Density	rho	21450[kg...	kg/m³
<input checked="" type="checkbox"/>	Thermal conductivity	k_iso ;...	71.6[W/(...	W/(m·K)
<input checked="" type="checkbox"/>	Relative permittivity	epsilon...	0.998	1
	Coefficient of thermal expansion	alpha_i...	8.80e-6[1...	1/K
	Young's modulus	E	168e9[Pa]	Pa
	Poisson's ratio	nu	0.38	1

Platinum

»	Property	Variable	Value	Unit
<input checked="" type="checkbox"/>	Electrical conductivity	sigma...	45.6e6[S...	S/m
<input checked="" type="checkbox"/>	Heat capacity at constant pres...	Cp	129[J/(k...	J/(kg·K)
<input checked="" type="checkbox"/>	Density	rho	19300[k...	kg/m³
<input checked="" type="checkbox"/>	Thermal conductivity	k_iso ;...	317[W/(...	W/(m·K)
<input checked="" type="checkbox"/>	Relative permittivity	epsilo...	1	1
	Coefficient of thermal expansi...	alpha_...	14.2e-6[...	1/K
	Young's modulus	E	70e9[Pa]	Pa
	Poisson's ratio	nu	0.44	1

Gold

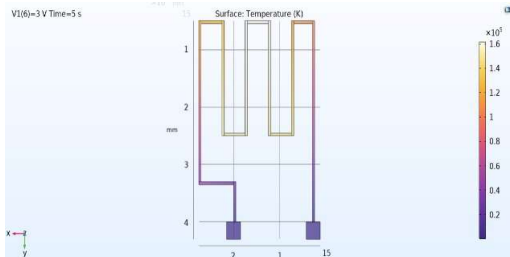
»	Property	Variable	Value	Unit
<input checked="" type="checkbox"/>	Electrical conductivity	sigma...	61.6e6[S...	S/m
<input checked="" type="checkbox"/>	Heat capacity at constant pres...	Cp	235[J/(k...	J/(kg·K)
<input checked="" type="checkbox"/>	Density	rho	10500[k...	kg/m³
<input checked="" type="checkbox"/>	Thermal conductivity	k_iso ;...	429[W/(...	W/(m·K)
<input checked="" type="checkbox"/>	Relative permittivity	epsilo...	-15.293	1
	Coefficient of thermal expansi...	alpha_...	18.9e-6[...	1/K
	Young's modulus	E	83e9[Pa]	Pa
	Poisson's ratio	nu	0.37	1

Silver

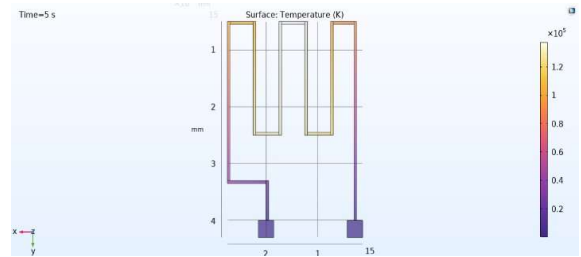
Chapter 5

Heater Simulations

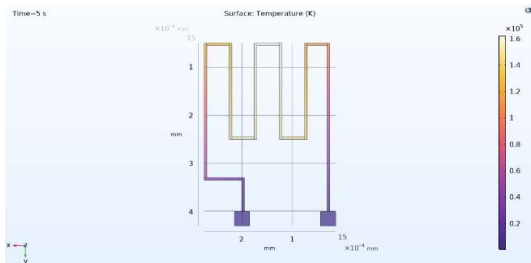
1) Meander Geometry



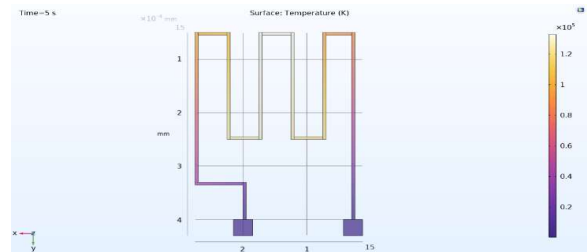
Material – Ag



Material-Pt

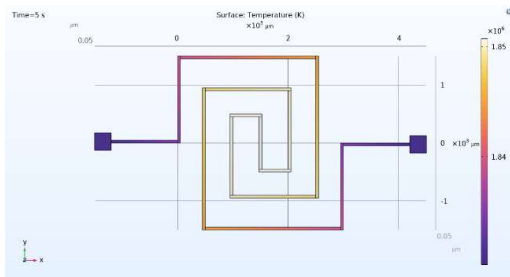


Material – Au

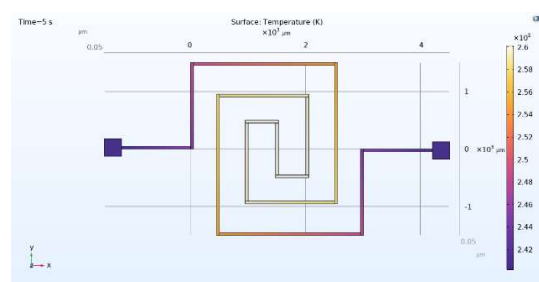


Material – Pd

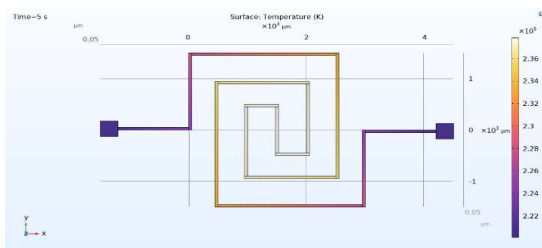
2) Spiral Geometry



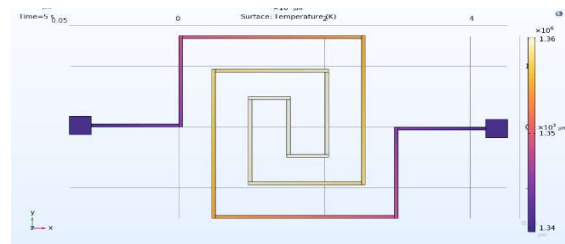
Material – Ag



Material – Pd

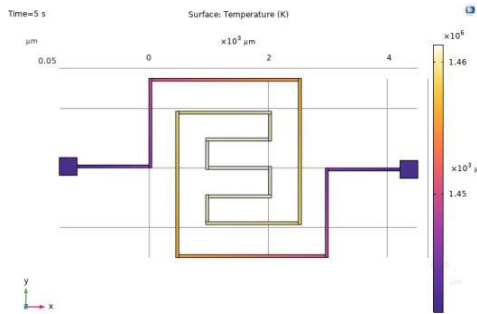


Material – Pt

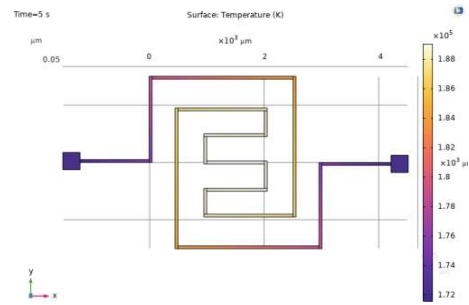


Material – Au

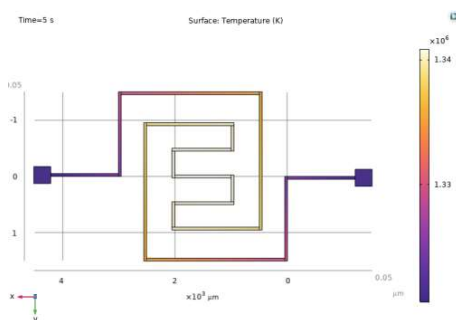
3) Spiral Meander Geometry



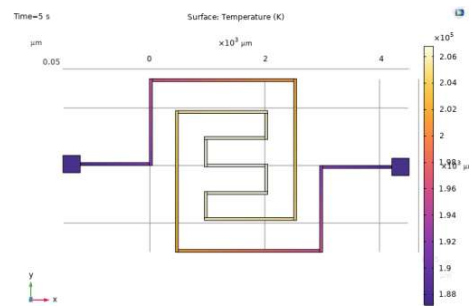
Material – Ag



Material – Pt

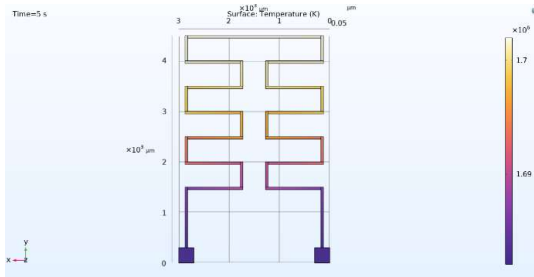


Material – Au

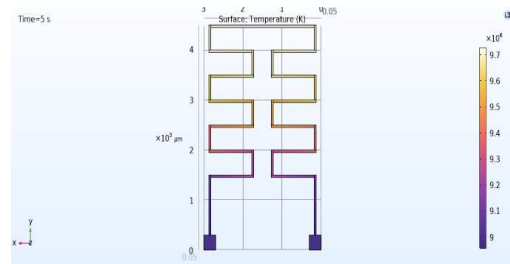


Material – Pd

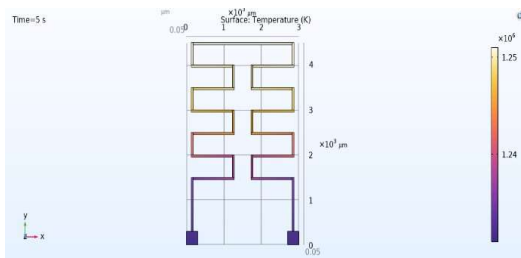
4) Double Meander Geometry



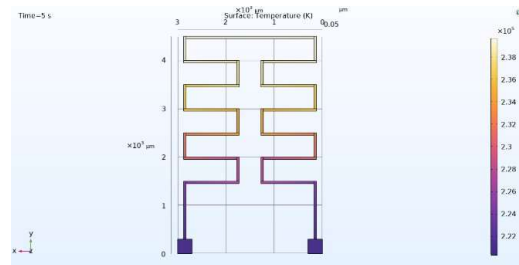
Material – Ag



Material – Pt

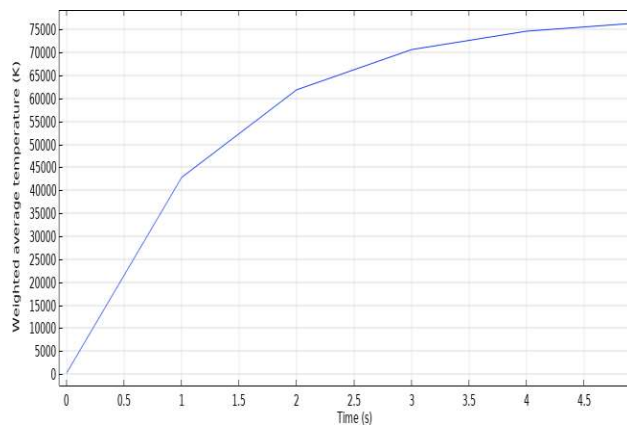


Material - Au

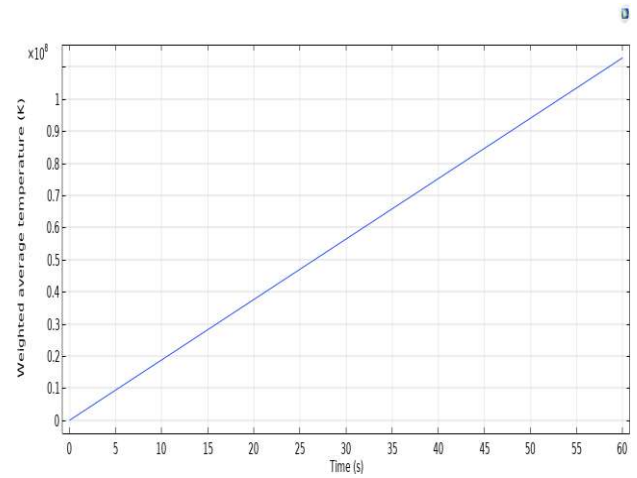


Material -Pd

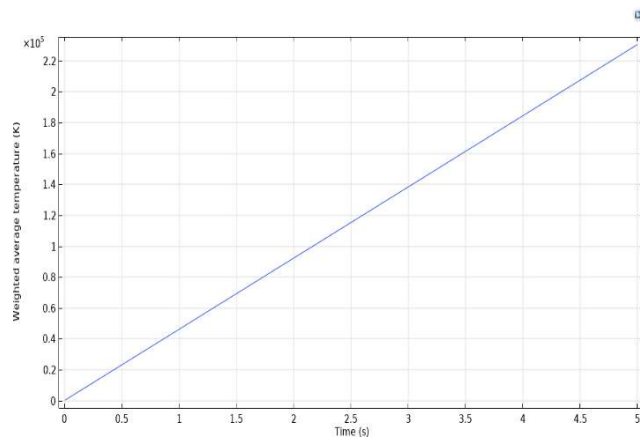
Graph Simulation for Pt material



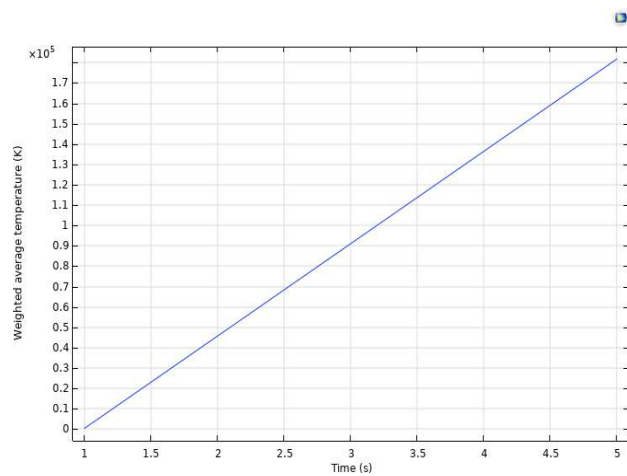
Meander Geometry



Double Meander Geometry



Spiral Geometry



Spiral Meander Geometry

Chapter 6

Why use platinum?

Platinum has various beneficial qualities, which make it a common material for micro heater geometries in gas sensors.

1.High Temperature Stability: Micro heaters that must function in challenging conditions with significant temperature fluctuations must have platinum's exceptional stability at high temperatures.

2.Low Reactivity: At normal operating temperatures, platinum is relatively inert, meaning that it doesn't react easily with gasses or other compounds. Over time, this inertness aids in preserving the integrity of the sensor's performance.

3.Excellent Electrical Conductivity: Micro heaters depend on electrical resistance to produce heat effectively, hence platinum's ability to conduct electricity is crucial.

4.Oxidation Resistance: Even at high temperatures, platinum exhibits remarkable resistance to oxidation. This feature is essential for gas sensors since the material may eventually deteriorate in the presence of oxygen or other oxidizing gases.

5.Compatibility with Semiconductor Processing: Platinum is a suitable candidate for fabrication because it is easily incorporated into semiconductor manufacturing processes that are frequently utilized to build microelectromechanical systems (MEMS) and other micro-scale devices.

6.Temperature Coefficient of Resistance: The calibration and operation of micro heater-based gas sensors are made easier by the relatively linear temperature coefficient of resistance of platinum over a broad temperature range.

Chapter 7

Interdigital Electrodes(IDEs)

Interdigital electrodes, or IDEs for short, are an electrode design that is widely utilized in a variety of sensing and actuation applications, especially in the fields of microfluidics and microelectromechanical systems (MEMS). These electrodes have an interdigitated pattern thanks to their comb-like architecture, which features finger-like structures extending from opposite sides. Interdigital electrodes' primary function is to increase sensors' and actuators' sensitivity, especially in capacitive sensing applications. The electrodes' surface area is increased by the interdigital design, which expands the area in which the electrode and the sensing material can interact. Because of its larger surface area, which boosts detection sensitivity, this technology is very helpful for a variety of sensing applications, including chemical, gas, humidity, and biosensors. When a gas sensor is exposed to a gas, the IDEs can be used to measure the change in resistance of the sensing material.

Interdigital electrodes are frequently made from metals including gold (Au), silver (Ag), and platinum (Pt) because of their superior conductivity, resistance to corrosion, and biocompatibility. The material used here for IDEs is gold(Au).

Chapter 8

Sensing Layer

Due to its unique characteristics, aluminum-doped zinc oxide (AZO) and zinc oxide (ZnO) have become attractive options for gas sensors. Because of its exceptional stability and sensitivity, ZnO is widely used in environmental monitoring for the detection of gases including CO, VOCs, NH₃, and NO₂. On the other hand, AZO performs better in terms of sensor response times and selectivity thanks to increased electrical conductivity brought about by aluminum doping. Both materials are compatible with different substrates, therefore they may be integrated into different kinds of sensor structures. The use of functionalization for improved selectivity and nanostructures to increase surface area are recent developments. The creation of flexible, wearable sensors and integration with the Internet of Things (IoT) highlight the adaptability of ZnO and AZO in smart sensing applications. Nevertheless, issues like cross-sensitivity and stability in challenging environments still exist, which spurs continued research to get around these restrictions. All things considered, the ongoing developments in ZnO and AZO sensing layers show promise for the development of more effective and adaptable gas sensors, which could have an impact on industrial safety, healthcare, and environmental monitoring.

Chapter 9

Velocity profile of Gas Chamber

A MEMS (Micro-Electro-Mechanical Systems) gas chamber's velocity profile is determined by a number of variables, including the geometry of the chamber, the type of flow (turbulent or laminar), and any applied forces or boundary conditions. Generally speaking, several flow regimes, such as laminar, transitional, or turbulent flow, can be used to characterize the velocity profile in a gas chamber.

Laminar flow is used in the gas chamber simulation. In a laminar flow, the gas flows in parallel, smooth layers with little mixing in between them. The velocity profile usually exhibits a parabolic distribution, wherein the centre of the chamber experiences the highest velocity, which subsequently decreases towards the walls. Poiseuille's law describes this behaviour, and analytical solutions for basic geometries can be used to compute the velocity profile.

Inlet pressure : 0.1Pa

Inlet concentration : 1mol/m³

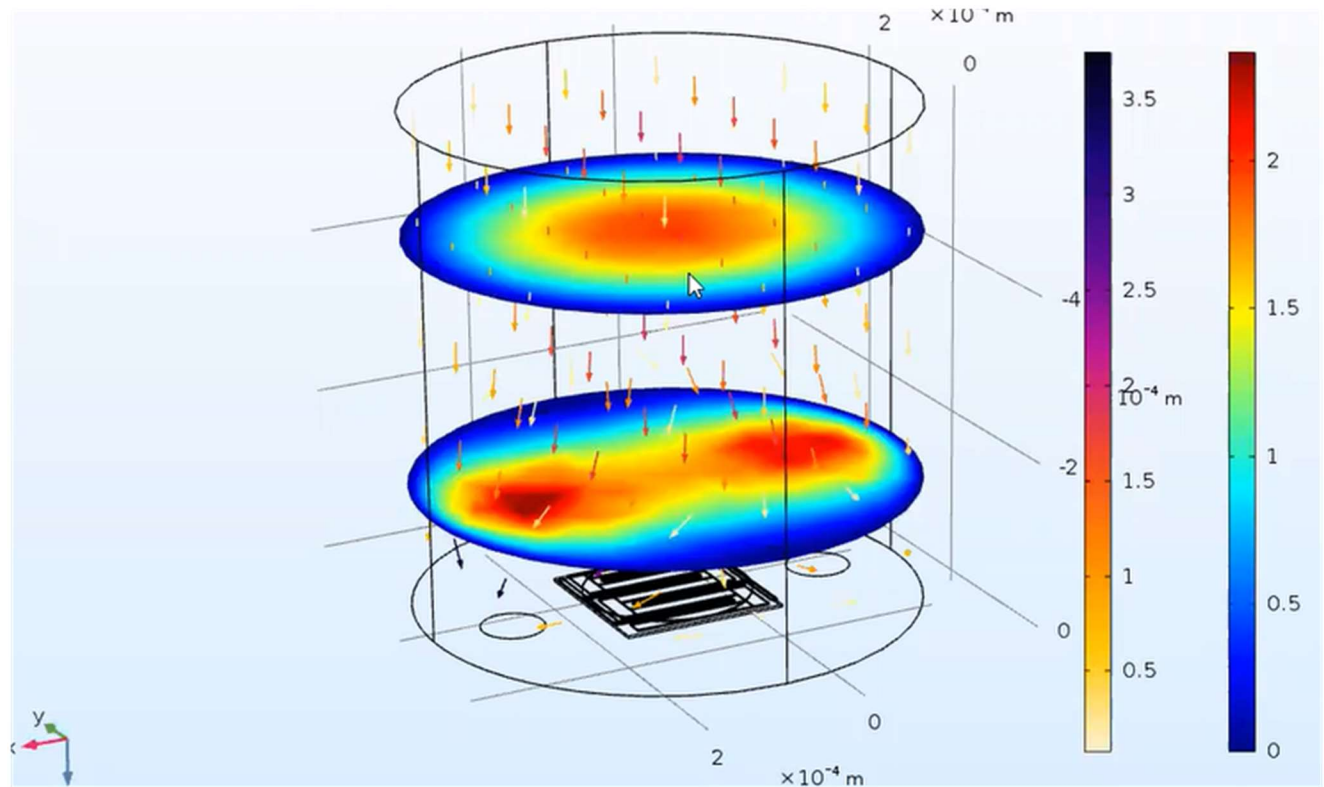


Fig. No.12: Velocity and concentration profile of NO₂ gas flow in simulation environment.

Velocity profile with heater working:

When a MEMS heater operates within a gas chamber, it alters the velocity profile of the gas flow due to thermal interactions. The activation of the heater produces heat, which causes the surrounding gas to expand thermally and alter its viscosity and density. As a result, there may be a shift in the velocity profile near the heater. In addition, the heated gas may create buoyancy effects, which could result in convection currents inside the chamber and affect the velocity distribution even more, especially in areas close to the heater. The heater's temperature gradients produce thermal driving forces that have the ability to propel gas flow through natural convection mechanisms. The boundary layer close to the chamber walls is impacted by these variables combined, which modifies the overall velocity profile.

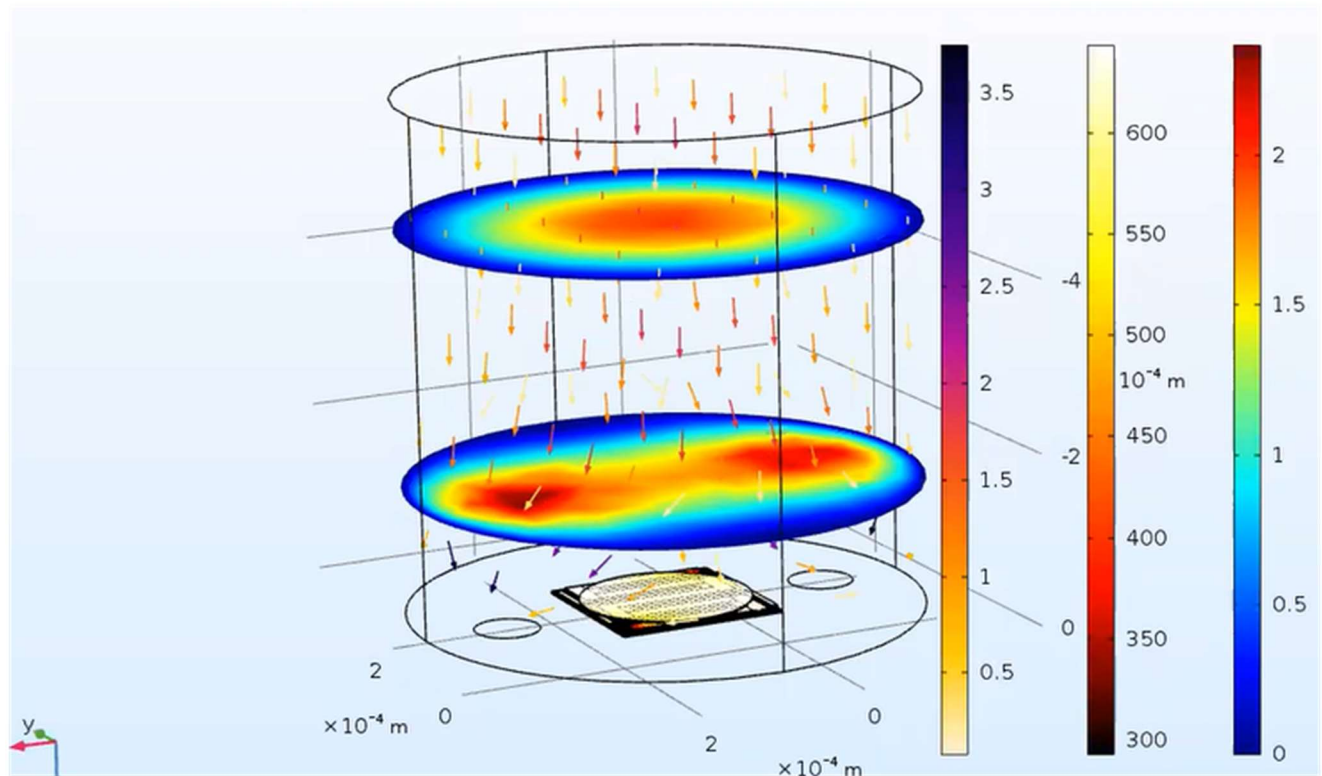


Fig. No.13: Velocity and concentration profile of NO2 gas with heater engaged.

Chapter 10

IOT Implementation of gas sensor

The development of an Internet of Things (IoT) device for gas monitoring is done by integrating a NodeMCU microcontroller with an MQ-135 gas sensor using the Blynk platform. Main process involved are the integration process, including hardware connections, software setup, and the role of each component in creating a functional IoT device.

The use of Internet of Things (IoT) technology has completely changed how we gather, process, and use real-time data from physical items. IoT is widely used in environmental monitoring, where sensors are used to evaluate air quality among other metrics. In order to develop an Internet of Things device that can monitor gas concentrations, we will primarily concentrate on the integration of a NodeMCU microcontroller with a MQ-135 gas sensor. Through communication with the Blynk platform, the gadget allows for remote control and data display.

Background:

- NodeMCU: The ESP8266 Wi-Fi module serves as the foundation for this open-source development board. Its GPIO pins and integrated Wi-Fi capabilities make it a strong foundation for Internet of Things projects.
- MQ-135 Gas Sensor: This well-liked gas sensor can identify a variety of gases, such as carbon dioxide, ammonia, and benzene. The notion of resistance changes in response to the concentration of target gases underlies its operation.
- Blynk Platform: This adaptable Internet of Things platform enables users to create personalized dashboards and control interfaces for linked gadgets. It is perfect for IoT projects because it supports multiple hardware platforms and offers cloud connectivity.

Integration Process:

Both hardware and software components are needed to integrate the NodeMCU with the MQ-135 gas sensor.

- Hardware Connections: The required power supply connections are made, and the MQ-135 sensor is linked to the analog pin of the NodeMCU. In addition, a resistor is utilized for voltage division in order to interface the sensor's analog output with the NodeMCU.
- Software Configuration: The Arduino IDE is used to program the NodeMCU firmware, which includes libraries for interacting with the MQ-135 sensor and connecting to the Blynk platform. In order to interpret sensor outputs, data conversion techniques are applied and calibration procedures are carried out to guarantee reliable sensor readings.

Blynk Integration:

Blynk Project Setup: An authentication token is obtained and a Blynk project is formed. This allows the NodeMCU and the Blynk server to communicate with each other.

- NodeMCU Configuration: Using the supplied authentication token, the NodeMCU firmware is set up to connect to the Wi-Fi network and establish a connection with the Blynk server.
- Data Transmission: The NodeMCU gathers sensor data, which is transmitted to the Blynk cloud

platform. From there, it can be seen in real-time on the Blynk dashboard through configurable widgets.

Role as an IoT Device:

The put together system serves as a complete gas monitoring IoT device, with the following features available:

- Sensing: The MQ-135 sensor provides real-time data on gas concentrations to the NodeMCU.
- Connectivity: The NodeMCU connects to the Blynk cloud platform via Wi-Fi connectivity, allowing for remote data transmission.
- Data Visualization: Customizable widgets on the Blynk dashboard allow real-time visualization of sensor data, enabling remote monitoring.
- alarms and Control: By using sensor readings, users can remotely control connected devices and set alarms based on predetermined criteria.

Applications and Significance:

Environmental Monitoring: In metropolitan contexts, air quality assessment and pollution source identification are greatly aided by Internet of Things (IoT) gas monitoring devices.

- Industrial Safety: By enabling early identification of dangerous gases, gas sensors coupled with IoT systems improve safety precautions in industrial settings.
- Smart Home Automation: By guaranteeing interior air quality and enabling energy-efficient ventilation, gas monitoring Internet of Things devices support smart home automation systems.

Code:

```
#define BLYNK_TEMPLATE_ID "TMPL3JL2Vj8aj"
#define BLYNK_TEMPLATE_NAME "Gas Sensor"
#define BLYNK_AUTH_TOKEN "ZrgvuF0l1m5sBI2CDSmW5gKuIqaohHLJ"
#include <ESP8266WiFi.h>

#include <BlynkSimpleEsp8266.h>

// WiFi credentials
char ssid[] = "realme";
char pass[] = "tejasviaryaa";

// Blynk auth token
char auth[] = BLYNK_AUTH_TOKEN;

// Sensor pin - adjust the pin according to your connection
int sensorPin = A0; // Analog pin where the gas sensor is connected

void setup() {
  Serial.begin(9600); // Start serial communication at 9600 baud rate
  Blynk.begin(auth, ssid, pass); // Connect to Blynk
```

```

}

void loop() {
  int sensorValue = analogRead(sensorPin); // Read the gas sensor value

  // Print the sensor value to the Serial Monitor
  Serial.print("Sensor Value: ");
  Serial.println(sensorValue);
  if (sensorValue > 300) {
    Blynk.logEvent("voltage_is_low");
  }
  // Send the sensor value to Blynk app on virtual pin V0
  Blynk.virtualWrite(V0, sensorValue);

  Blynk.run(); // Initiates Blynk
  delay(1000); // Wait for a second before reading again
}

```

Chapter 11

Fabricated Gas Sensor

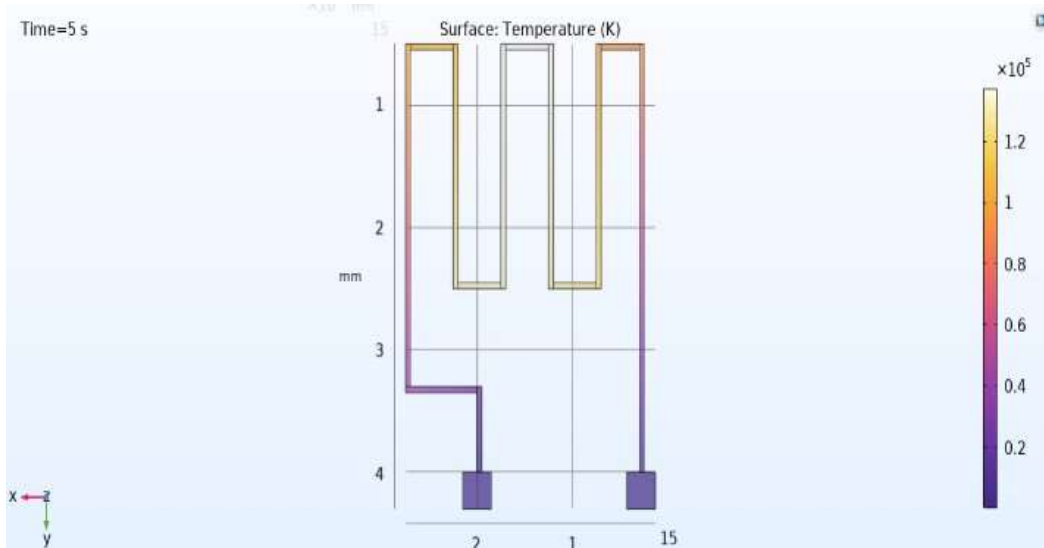


Fig.14: Meander Geometry used in fabricated sensor

Dimension: 3cmX3cm
Geometry: Meander
Heater Material: Platinum
IDE Material: Gold
Sensing layer: ZnO

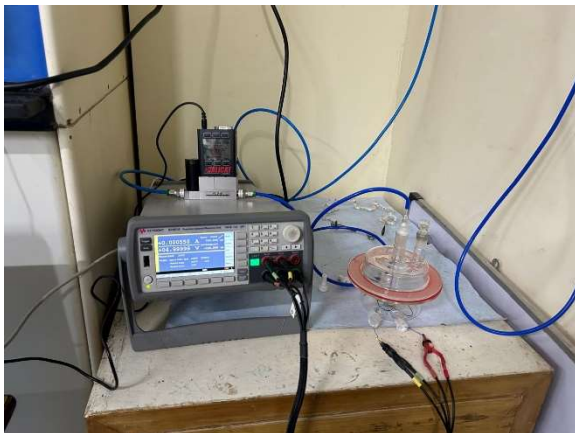


Image.1: Sensor testing

NO₂ gas of 5sccm concentration is passed over the gas sensor to obtain the following data of voltage input and current output.

Voltage	I1	I2		Voltage	I1	I2		Voltage	I1	I2
-5	-3.46E-04	-3.58E-04		-3.35655	-1.99E-04	-2.09E-04		-1.7131	-5.20E-05	-6.00E-05
-4.97215	-3.41E-04	-3.58E-04		-3.3287	-1.98E-04	-2.06E-04		-1.68524	-4.60E-05	-4.90E-05
-4.9443	-3.41E-04	-3.59E-04		-3.30084	-1.91E-04	-2.03E-04		-1.65739	-4.60E-05	-5.30E-05
-4.91644	-3.39E-04	-3.50E-04		-3.27299	-1.90E-04	-2.01E-04		-1.62953	-4.10E-05	-4.70E-05
-4.88859	-3.33E-04	-3.51E-04		-3.24513	-1.90E-04	-1.96E-04		-1.60168	-4.20E-05	-4.60E-05
-4.86073	-3.36E-04	-3.50E-04		-3.21728	-1.87E-04	-1.94E-04		-1.57382	-4.10E-05	-4.30E-05
-4.83287	-3.35E-04	-3.47E-04		-3.18942	-1.84E-04	-1.91E-04		-1.54597	-3.90E-05	-4.00E-05
-4.80502	-3.32E-04	-3.40E-04		-3.16157	-1.80E-04	-1.87E-04		-1.51811	-3.30E-05	-3.60E-05
-4.77717	-3.29E-04	-3.44E-04		-3.13371	-1.76E-04	-1.83E-04		-1.49026	-3.20E-05	-3.20E-05
-4.74931	-3.20E-04	-3.38E-04		-3.10585	-1.75E-04	-1.87E-04		-1.4624	-3.00E-05	-3.00E-05
-4.72145	-3.17E-04	-3.37E-04		-3.078	-1.68E-04	-1.84E-04		-1.43455	-2.70E-05	-2.50E-05
-4.6936	-3.19E-04	-3.29E-04		-3.05015	-1.74E-04	-1.78E-04		-1.40669	-2.40E-05	-2.40E-05
-4.66574	-3.19E-04	-3.30E-04		-3.02229	-1.68E-04	-1.76E-04		-1.37884	-2.30E-05	-2.50E-05
-4.63789	-3.16E-04	-3.27E-04		-2.99444	-1.70E-04	-1.79E-04		-1.35098	-2.10E-05	-2.30E-05
-4.61004	-3.08E-04	-3.27E-04		-2.96658	-1.66E-04	-1.70E-04		-1.32313	-1.70E-05	-2.00E-05
-4.58218	-3.07E-04	-3.26E-04		-2.93872	-1.59E-04	-1.70E-04		-1.29527	-1.40E-05	-1.50E-05
-4.55433	-3.11E-04	-3.20E-04		-2.91087	-1.60E-04	-1.69E-04		-1.26742	-1.30E-05	-8.00E-06
-4.52647	-3.10E-04	-3.20E-04		-2.88302	-1.55E-04	-1.69E-04		-1.23956	-5.00E-06	-5.00E-06
-4.49861	-2.99E-04	-3.17E-04		-2.85516	-1.52E-04	-1.64E-04		-1.21171	-5.00E-06	-5.00E-06
-4.47076	-2.98E-04	-3.13E-04		-2.8273	-1.50E-04	-1.59E-04		-1.18385	-2.00E-06	-3.00E-06
-4.4429	-3.01E-04	-3.11E-04		-2.79945	-1.49E-04	-1.56E-04		-1.15599	2.00E-06	0
-4.41505	-2.94E-04	-3.07E-04		-2.7716	-1.45E-04	-1.54E-04		-1.12814	-2.00E-06	3.00E-06
-4.38719	-2.90E-04	-3.04E-04		-2.74374	-1.45E-04	-1.47E-04		-1.10029	-3.00E-06	4.00E-06
-4.35933	-2.93E-04	-3.04E-04		-2.71588	-1.40E-04	-1.44E-04		-1.07243	5.00E-06	5.00E-06
-4.33148	-2.85E-04	-3.03E-04		-2.68803	-1.33E-04	-1.43E-04		-1.04458	3.00E-06	9.00E-06
-4.30363	-2.82E-04	-3.00E-04		-2.66017	-1.35E-04	-1.42E-04		-1.01672	9.00E-06	1.20E-05
-4.27577	-2.81E-04	-2.96E-04		-2.63231	-1.31E-04	-1.38E-04		-0.98886	1.10E-05	1.40E-05
-4.24792	-2.78E-04	-2.93E-04		-2.60446	-1.34E-04	-1.37E-04		-0.96101	1.30E-05	1.60E-05
-4.22006	-2.78E-04	-2.88E-04		-2.57661	-1.27E-04	-1.33E-04		-0.93315	1.10E-05	1.80E-05
-4.1922	-2.76E-04	-2.85E-04		-2.54875	-1.27E-04	-1.35E-04		-0.9053	1.70E-05	2.60E-05
-4.16435	-2.73E-04	-2.87E-04		-2.5209	-1.21E-04	-1.32E-04		-0.87744	2.10E-05	2.40E-05
-4.1365	-2.63E-04	-2.81E-04		-2.49304	-1.24E-04	-1.30E-04		-0.84959	2.70E-05	2.60E-05
-4.10864	-2.64E-04	-2.83E-04		-2.46519	-1.19E-04	-1.27E-04		-0.82173	2.90E-05	2.90E-05
-4.08078	-2.64E-04	-2.76E-04		-2.43733	-1.14E-04	-1.21E-04		-0.79388	2.70E-05	3.00E-05
-4.05293	-2.56E-04	-2.74E-04		-2.40948	-1.12E-04	-1.19E-04		-0.76602	3.30E-05	3.50E-05
-4.02508	-2.56E-04	-2.72E-04		-2.38162	-1.06E-04	-1.18E-04		-0.73817	3.00E-05	3.60E-05
-3.99722	-2.53E-04	-2.65E-04		-2.35376	-1.04E-04	-1.17E-04		-0.71031	3.90E-05	4.00E-05
-3.96936	-2.51E-04	-2.63E-04		-2.32591	-1.08E-04	-1.15E-04		-0.68246	3.70E-05	3.90E-05
-3.94151	-2.48E-04	-2.61E-04		-2.29806	-1.06E-04	-1.06E-04		-0.6546	3.80E-05	4.60E-05
-3.91365	-2.48E-04	-2.59E-04		-2.2702	-1.04E-04	-1.09E-04		-0.62675	4.20E-05	5.00E-05
-3.8858	-2.46E-04	-2.54E-04		-2.24235	-1.00E-04	-1.02E-04		-0.59889	4.80E-05	5.20E-05
-3.85795	-2.43E-04	-2.57E-04		-2.21449	-9.50E-05	-1.00E-04		-0.57104	4.80E-05	5.90E-05
-3.83009	-2.42E-04	-2.56E-04		-2.18664	-9.50E-05	-9.70E-05		-0.54318	5.10E-05	5.70E-05
-3.80223	-2.37E-04	-2.51E-04		-2.15878	-8.90E-05	-9.20E-05		-0.51533	4.90E-05	5.70E-05
-3.77438	-2.34E-04	-2.47E-04		-2.13093	-8.90E-05	-9.40E-05		-0.48747	6.00E-05	6.00E-05
-3.74653	-2.28E-04	-2.43E-04		-2.10307	-8.50E-05	-9.00E-05		-0.45962	6.20E-05	6.10E-05
-3.71867	-2.27E-04	-2.42E-04		-2.07521	-8.30E-05	-8.70E-05		-0.43176	5.90E-05	6.20E-05
-3.69081	-2.26E-04	-2.35E-04		-2.04736	-7.70E-05	-8.50E-05		-0.4039	5.90E-05	6.80E-05
-3.66296	-2.27E-04	-2.32E-04		-2.01951	-7.60E-05	-8.10E-05		-0.37605	6.60E-05	6.90E-05
-3.6351	-2.28E-04	-2.38E-04		-1.99165	-7.70E-05	-8.10E-05		-0.34819	7.00E-05	7.20E-05
-3.60725	-2.22E-04	-2.35E-04		-1.9638	-7.20E-05	-7.70E-05		-0.32034	7.10E-05	7.40E-05
-3.57939	-2.22E-04	-2.31E-04		-1.93594	-6.80E-05	-7.30E-05		-0.29248	7.50E-05	7.40E-05
-3.55154	-2.14E-04	-2.26E-04		-1.90808	-6.70E-05	-7.20E-05		-0.26463	7.30E-05	7.70E-05
-3.52368	-2.17E-04	-2.25E-04		-1.88023	-6.30E-05	-6.90E-05		-0.23677	7.80E-05	7.80E-05
-3.49583	-2.13E-04	-2.22E-04		-1.85238	-6.00E-05	-6.80E-05		-0.20892	8.30E-05	8.20E-05
-3.46797	-2.09E-04	-2.24E-04		-1.82452	-6.20E-05	-6.80E-05		-0.18106	8.10E-05	8.70E-05
-3.44012	-2.08E-04	-2.18E-04		-1.79666	-5.90E-05	-5.90E-05		-0.15321	8.80E-05	8.80E-05
-3.41226	-2.03E-04	-2.13E-04		-1.76881	-5.80E-05	-5.90E-05		-0.12535	8.30E-05	9.30E-05
-3.38441	-1.99E-04	-2.10E-04		-1.74095	-5.10E-05	-5.90E-05		-0.0975	9.20E-05	9.80E-05

Voltage	I1	I2		Voltage	I1	I2		Voltage	I1	I2
-0.06964	9.10E-05	9.80E-05		1.57381	2.42E-04	2.52E-04		3.21726	3.95E-04	4.05E-04
-0.04179	9.60E-05	1.00E-04		1.60167	2.44E-04	2.46E-04		3.24512	3.98E-04	4.06E-04
-0.01393	9.80E-05	9.80E-05		1.62952	2.50E-04	2.56E-04		3.27298	3.99E-04	4.09E-04
0.01392	1.00E-04	1.03E-04		1.65738	2.53E-04	2.57E-04		3.30083	4.01E-04	4.10E-04
0.04178	1.00E-04	1.07E-04		1.68523	2.56E-04	2.57E-04		3.32869	4.06E-04	4.12E-04
0.06963	1.01E-04	1.11E-04		1.71309	2.57E-04	2.60E-04		3.35654	4.02E-04	4.19E-04
0.09749	1.07E-04	1.11E-04		1.74094	2.59E-04	2.65E-04		3.38439	4.09E-04	4.19E-04
0.12534	1.12E-04	1.14E-04		1.76879	2.65E-04	2.68E-04		3.41225	4.10E-04	4.24E-04
0.1532	1.15E-04	1.17E-04		1.79665	2.65E-04	2.69E-04		3.44011	4.12E-04	4.29E-04
0.18105	1.13E-04	1.16E-04		1.82451	2.67E-04	2.75E-04		3.46796	4.18E-04	4.32E-04
0.20891	1.16E-04	1.22E-04		1.85236	2.68E-04	2.72E-04		3.49581	4.19E-04	4.35E-04
0.23676	1.20E-04	1.22E-04		1.88022	2.70E-04	2.73E-04		3.52367	4.20E-04	4.34E-04
0.26462	1.26E-04	1.29E-04		1.90807	2.70E-04	2.77E-04		3.55152	4.23E-04	4.31E-04
0.29247	1.29E-04	1.29E-04		1.93593	2.71E-04	2.80E-04		3.57938	4.28E-04	4.39E-04
0.32033	1.31E-04	1.34E-04		1.96378	2.79E-04	2.88E-04		3.60724	4.28E-04	4.39E-04
0.34818	1.39E-04	1.39E-04		1.99164	2.83E-04	2.86E-04		3.63509	4.34E-04	4.40E-04
0.37604	1.36E-04	1.39E-04		2.01949	2.84E-04	2.90E-04		3.66295	4.37E-04	4.46E-04
0.4039	1.37E-04	1.40E-04		2.04735	2.84E-04	2.97E-04		3.6908	4.37E-04	4.48E-04
0.43175	1.42E-04	1.45E-04		2.0752	2.87E-04	2.96E-04		3.71866	4.46E-04	4.58E-04
0.4596	1.40E-04	1.46E-04		2.10306	2.93E-04	2.96E-04		3.74651	4.44E-04	4.55E-04
0.48746	1.41E-04	1.46E-04		2.13092	2.96E-04	3.01E-04		3.77437	4.45E-04	4.53E-04
0.51531	1.51E-04	1.45E-04		2.15877	2.98E-04	3.03E-04		3.80222	4.52E-04	4.58E-04
0.54317	1.49E-04	1.52E-04		2.18662	2.98E-04	3.01E-04		3.83008	4.54E-04	4.59E-04
0.57102	1.55E-04	1.54E-04		2.21448	3.02E-04	3.10E-04		3.85793	4.60E-04	4.65E-04
0.59888	1.53E-04	1.53E-04		2.24233	3.01E-04	3.10E-04		3.88579	4.59E-04	4.66E-04
0.62673	1.58E-04	1.61E-04		2.27019	3.07E-04	3.13E-04		3.91364	4.61E-04	4.69E-04
0.65459	1.60E-04	1.64E-04		2.29805	3.10E-04	3.18E-04		3.9415	4.61E-04	4.72E-04
0.68245	1.61E-04	1.71E-04		2.3259	3.12E-04	3.19E-04		3.96935	4.68E-04	4.70E-04
0.7103	1.61E-04	1.68E-04		2.35375	3.11E-04	3.23E-04		3.99721	4.66E-04	4.72E-04
0.73816	1.65E-04	1.70E-04		2.38161	3.22E-04	3.24E-04		4.02506	4.73E-04	4.76E-04
0.76601	1.69E-04	1.72E-04		2.40946	3.19E-04	3.28E-04		4.05292	4.73E-04	4.82E-04
0.79386	1.70E-04	1.77E-04		2.43732	3.19E-04	3.28E-04		4.08078	4.77E-04	4.88E-04
0.82172	1.76E-04	1.79E-04		2.46518	3.21E-04	3.37E-04		4.10863	4.79E-04	4.86E-04
0.84958	1.74E-04	1.82E-04		2.49303	3.23E-04	3.37E-04		4.13649	4.84E-04	4.86E-04
0.87743	1.80E-04	1.86E-04		2.52089	3.26E-04	3.43E-04		4.16434	4.85E-04	4.92E-04
0.90529	1.79E-04	1.87E-04		2.54874	3.31E-04	3.44E-04		4.19219	4.91E-04	4.94E-04
0.93314	1.84E-04	1.85E-04		2.5766	3.32E-04	3.48E-04		4.22005	4.88E-04	4.95E-04
0.96099	1.90E-04	1.89E-04		2.60445	3.39E-04	3.47E-04		4.2479	4.90E-04	5.00E-04
0.98885	1.87E-04	1.94E-04		2.63231	3.38E-04	3.52E-04		4.27576	4.95E-04	5.02E-04
1.01671	1.94E-04	1.92E-04		2.66016	3.45E-04	3.52E-04		4.30361	4.99E-04	5.06E-04
1.04456	1.92E-04	2.03E-04		2.68802	3.43E-04	3.55E-04		4.33147	5.02E-04	5.07E-04
1.07242	1.95E-04	2.05E-04		2.71587	3.50E-04	3.56E-04		4.35933	5.06E-04	5.07E-04
1.10027	2.01E-04	2.04E-04		2.74373	3.49E-04	3.61E-04		4.38718	5.06E-04	5.12E-04
1.12813	1.99E-04	2.10E-04		2.77158	3.53E-04	3.58E-04		4.41503	5.08E-04	5.17E-04
1.15598	2.06E-04	2.12E-04		2.79944	3.52E-04	3.62E-04		4.44289	5.16E-04	5.14E-04
1.18384	2.06E-04	2.19E-04		2.82729	3.54E-04	3.69E-04		4.47074	5.13E-04	5.21E-04
1.21169	2.10E-04	2.20E-04		2.85515	3.59E-04	3.70E-04		4.4986	5.14E-04	5.23E-04
1.23955	2.16E-04	2.22E-04		2.883	3.62E-04	3.73E-04		4.52646	5.22E-04	5.25E-04
1.2674	2.17E-04	2.26E-04		2.91085	3.66E-04	3.78E-04		4.55431	5.22E-04	5.29E-04
1.29526	2.16E-04	2.22E-04		2.93871	3.66E-04	3.82E-04		4.58217	5.23E-04	5.30E-04
1.32312	2.20E-04	2.26E-04		2.96657	3.65E-04	3.84E-04		4.61002	5.25E-04	5.35E-04
1.35097	2.25E-04	2.33E-04		2.99442	3.68E-04	3.86E-04		4.63787	5.24E-04	5.38E-04
1.37882	2.25E-04	2.31E-04		3.02228	3.71E-04	3.86E-04		4.66573	5.35E-04	5.42E-04
1.40668	2.29E-04	2.39E-04		3.05013	3.74E-04	3.94E-04		4.69359	5.38E-04	5.44E-04
1.43453	2.29E-04	2.41E-04		3.07799	3.83E-04	3.91E-04		4.72144	5.37E-04	5.49E-04
1.46239	2.30E-04	2.37E-04		3.10584	3.84E-04	3.98E-04		4.7493	5.42E-04	5.44E-04
1.49025	2.36E-04	2.43E-04		3.1337	3.83E-04	4.02E-04		4.77715	5.44E-04	5.52E-04
1.5181	2.37E-04	2.45E-04		3.16155	3.86E-04	4.00E-04		4.80501	5.47E-04	5.53E-04
1.54595	2.41E-04	2.48E-04		3.18941	3.92E-04	4.03E-04		4.83286	5.50E-04	5.54E-04

Fig 15: Voltage-Current data for NO₂ gas

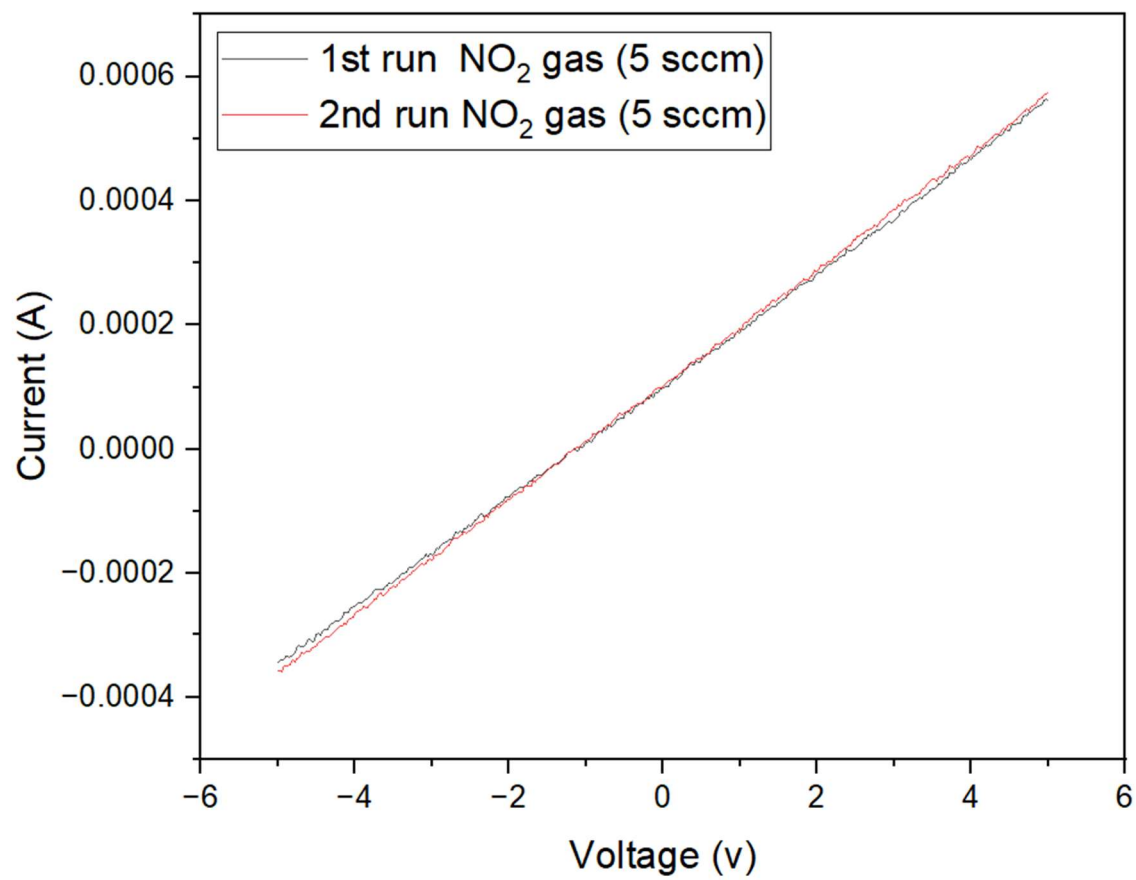


Fig.16: I vs V curve of fabricated gas sensor

Chapter 12

Conclusion

The project's primary objective is to design different geometries of micro-heaters for gas sensors that offer uniform heating while consuming minimal power. Different geometries affect microheater thermal efficiency. Optimal designs are required to improve energy efficiency that minimizes heat loss and maximizes heat generation. Lower power consumption and enhanced temperature control are essential for the reliable operation of micro-devices. The distribution and transfer of heat within the system are greatly affected by the micro heater's geometry.

Four geometries were designed and simulated on COMSOL software. Comparing spiral and meander spiral geometries to meander and double meander geometries with four different materials, it is discovered that the thermal homogeneity is better in the former case. At voltage of 3V , average and maximum temperatures are studied for the four different geometries with each of the four material.

The research also explores modifications to substrate, heater thickness and heating material parameters to improve micro-heater performance. However, further design optimization of the sensor may affect its sensitivity and selectivity differently.

The Blynk platform's integration of a NodeMCU microcontroller with a MQ-135 gas sensor shows how to create Internet of Things devices that are useful for gas monitoring applications. The system that has been put together takes advantage of the advantages that each component possesses to provide real-time data insights, remote accessibility, and control capabilities. This helps to meet the increasing need for environmental monitoring solutions across multiple industries. Promising opportunities exist for more research and development in this area to improve quality of life, sustainability, and safety.

References

- [1] S. Roy, T. Majhi, S. Sinha, C. K. Sarkar and H. Saha. "Electro thermal analysis and fabrication of low cost microheater using a nickel alloy for low temperature MEMS based gas sensor application." 2010 International Conference on Industrial Electronics, Control and Robotics. IEEE, 2010.
- [2] M. I. A. Asri, M. N. Hasan, M. R. A. Fuaad, Y. M. Yunus and M. S. M. Ali, "MEMS gas sensors: A review." IEEE Sensors Journal 21.17 (2021): 18381-18397
- [3] S. Bedoui, S. Gomri, H. Samet and A. Kachouri, "Design and electro-thermal analysis of a platinum micro heater for gas sensors." 2016 13th International Multi-Conference on Systems, Signals & Devices (SSD). IEEE, 2016.
- [4] C. Paun, R. Tomescu, D. Cristea, O. Ionescu and C. Parvulescu, "Design, fabrication and characterization of a micro-heater for metasurface-based gas sensors." 2020 International Semiconductor Conference (CAS). IEEE, 2020.
- [5] Joy, Steffy, and Jobin K. Antony. "Design and simulation of a micro hotplate using COMSOL multiphysics for MEMS based gas sensor." 2015 Fifth International Conference on Advances in Computing and Communications (ICACC). IEEE, 2015.
- [6] Nagirnyak, S. V., and T. A. Dontsova. "Gas sensor device creation." 2017 IEEE 7th International Conference Nanomaterials: Application & Properties (NAP). IEEE, 2017.
- [7] J. Wang, D. Yang, T. -L. Chang, P. Cui, Y. Duan and W. Ye, "Optimization Design of Flexible Gas Sensor Microheater." 2020 21st International Conference on Electronic Packaging Technology (ICEPT). IEEE, 2020.
- [8] Velmathi, G., N. Ramshanker, and S. Mohan. "2D Simulations and Electro-Thermal Analysis of Micro-Heater Designs Using COMSOL TM for Gas Sensor Applications." COMSOL Conference I. 2010.
- [9] Li, T., Xu, L., Wang, Y. (2017). Micro-heater-Based Gas Sensors. In: Huang, QA. (eds) Micro Electro Mechanical Systems. Micro/Nano Technologies, vol 2. Springer, Singapore. https://doi.org/10.1007/978-981-10-2798-7_21-1
- [10] Kathirvelan, J., and R. Vijayaraghavan. "Design, Simulation and Analysis of platinum micro heaters on Al₂O₃ substrate for sensor applications." ARPN Journal of Engineering and Applied Sciences 9.11 (2014): 2307-2314.
- [11] Jeroish, Z. E., K S Bhuvaneshwari "Microheater: material, design, fabrication, temperature control, and applications—a role in COVID-19." Biomedical microdevices 24 (2022): 1-49.

[12] Prasad, Mahanth, Neha Arora, and V. K. Khanna. "Design, Simulation and Fabrication of Platinum based Micro-heater for Gas Sensing Application." (2013)

ORIGINALITY REPORT

13%

SIMILARITY INDEX

6%

INTERNET SOURCES

10%

PUBLICATIONS

0%

STUDENT PAPERS

PRIMARY SOURCES

1	Wang, Shuqi. "Functional Regression Models for Gene-Based Association Analysis of Complex Traits.", Georgetown University, 2023 Publication	2%
2	www.electronicclinic.com Internet Source	1%
3	www.coursehero.com Internet Source	1%
4	manugupta-ai.com Internet Source	1%
5	B. A. Sawyerr, M. M. Ali, A. O. Adewumi. "A comparative study of some real-coded genetic algorithms for unconstrained global optimization", Optimization Methods and Software, 2011 Publication	<1%
6	Carlos Santos. "Efeitos dinâmicos induzidos por tráfego em atravessamentos inferiores pré-fabricados a vias de alta velocidade",	<1%

7

Gurdeep Singh, Urvinder Singh. "Hybrid binary grey wolf naked mole-rat algorithm for fragment-type UWB antenna optimization using time-varying transfer functions", Expert Systems with Applications, 2023

Publication

<1 %

8

Ay, Zeynep. "Development of Nano-Material Based Optical Chemical Sensors Indicating Oxygen Levels in Petrochemistry Related Workplaces", Dokuz Eylul Universitesi (Turkey), 2024

Publication

<1 %

9

D. Bortis, J. Biela, J.W. Kolar. "Active gate control for current balancing in parallel connected IGBT modules in solid state modulators", 2007 16th IEEE International Pulsed Power Conference, 2007

Publication

<1 %

10

Nandini G. Iyer, S. Suganthi, M. Arulmozhi, P. Sivakumar, S. Jeny Sophia. "Design and evaluation of micro-heater geometries for MEMS-based ozone gas sensor through a theoretical modeling", Materials Today: Proceedings, 2022

Publication

<1 %

11

subscription.packtpub.com

Internet Source

<1 %

12

Ruiqi Song, Weike Nie, Aiqin Hou, Suqin Xue.
"Dynamic random mutation hybrid Harris
hawk optimization and its application to
training kernel extreme learning machine",
Cluster Computing, 2024

Publication

<1 %

13

www.freepatentsonline.com

Internet Source

<1 %

14

Clark, Caelen Matthew. "Electrochemical
Methods for Biofilm Detection and
Characterization of Electrically Stimulated
Orthopedic Biomaterials.", State University of
New York at Buffalo, 2020

Publication

<1 %

15

John N. Bahcall. "Solar models with helium
and heavy-element diffusion", Reviews of
Modern Physics, 10/1995

Publication

<1 %

16

Abdulkarim, Salihu Aish. "Time Series
Forecasting using Dynamic Particle Swarm
Optimizer Trained Neural Networks",
University of Pretoria (South Africa), 2023

Publication

<1 %

17

K. Arun, M.S. Lekshmi, K.J. Suja. "Design and
Simulation of ZnO based Acetone Gas Sensor

<1 %

using COMSOL Multiphysics", 2020 7th International Conference on Signal Processing and Integrated Networks (SPIN), 2020

Publication

18

M. Senthil Arumugam. "A new and improved version of particle swarm optimization algorithm with global-local best parameters", Knowledge and Information Systems, 09/2008

Publication

<1 %

19

Sierra Rayne, Kaya Forest. "Ionization effects on the partitioning behavior of food and beverage aroma compounds between aqueous phases and air and organic matrices", Nature Precedings, 2011

Publication

<1 %

20

link.springer.com

Internet Source

<1 %

21

Gang Hu, Rui Yang, Guo Wei. "Hybrid chameleon swarm algorithm with multi-strategy: A case study of degree reduction for disk Wang-Ball curves", Mathematics and Computers in Simulation, 2023

Publication

<1 %

22

Aiouache, F.. "Liquid-liquid equilibria of ternary 2M1B/2M2B-2M1BOH-H²O and quaternary 2M1B-2M2B-2M1BOH-H²O mixtures", Fluid Phase Equilibria, 20010915

<1 %

23

Ammara Mehmood, Aneela Zameer, Naveed Ishtiaq Chaudhary, Muhammad Asif Zahoor Raja. "Backtracking search heuristics for identification of electrical muscle stimulation models using Hammerstein structure", Applied Soft Computing, 2019

Publication

<1 %

24

D. Yamashita, T. Niimura, R. Yokoyama, Y. Nakanishi. "Thermal unit scheduling for CO2 reduction including significant wind power penetration", 2011 IEEE Power and Energy Society General Meeting, 2011

Publication

<1 %

25

Dongcheng Xie, Dongliang Chen, Shufeng Peng, Yujie Yang, Lei Xu, Feng Wu. "A Low Power Cantilever-Based Metal Oxide Semiconductor Gas Sensor", IEEE Electron Device Letters, 2019

Publication

<1 %

26

Lee Florea, Ferenc L. Forray, Sarah M. Banks. "Chapter 4 Water Isotopes, Carbon Exports, and Landscape Evolution in the Vadu Crișului Karst Basin of Transylvania, Romania", Springer Science and Business Media LLC, 2020

Publication

<1 %

27	M.S. Lekshmi, K. Arun, K.J. Suja. "Design and Simulation of Metal Oxide Gas Sensor for Breath Analyzer Application", Key Engineering Materials, 2021 Publication	<1 %
28	Robert A. Toth. "Line strengths (900–3600 cm ^{−1}), self-broadened linewidths, and frequency shifts (1800–2360 cm ^{−1}) of N ₂ O", Applied Optics, 12/20/1993 Publication	<1 %
29	Zhang, H.. "Collision strengths and oscillator strengths for excitation to the n = 3 and 4 levels of neon-like ions", Atomic Data and Nuclear Data Tables, 198707 Publication	<1 %
30	dspace.aus.edu:8443 Internet Source	<1 %
31	www.researchgate.net Internet Source	<1 %
32	"Radiation Data", Annals of the ICRP, 2018 Publication	<1 %
33	"Technology Innovation in Mechanical Engineering", Springer Science and Business Media LLC, 2022 Publication	<1 %

34

Adachi, . "METAL AND SEMIMETAL ELEMENTS", The Handbook on Optical Constants of Metals In Tables and Figures, 2012.

Publication

<1 %

35

Arena, Kourtney N.. "Estimating the Impact of Intersection Traffic on Air Quality Emissions at Camden Cooper Medical Health Intersection Through the Integration of Vissim/Moves Models", Rowan University, 2023

Publication

<1 %

36

Chen, Yulong. "Design and Fabrication of MEMS Microheater and Its Application in Gas Sensing", University of Macau, 2023

Publication

<1 %

37

Chengyang Wang, Jiandong Jin, Yuling Li, Wenbo Ding, Mingjun Dai. " Design and fabrication of a MEMS-based gas sensor containing WO sensitive layer for detection of NO ", Journal of Micro/Nanolithography, MEMS, and MOEMS, 2017

Publication

<1 %

38

Christian L. M uller, Benedikt Baumgartner, Ivo F. Sbalzarini. "Particle Swarm CMA Evolution Strategy for the optimization of multi-funnel landscapes", 2009 IEEE Congress on Evolutionary Computation, 2009

Publication

<1 %

39	Smith, Matthew Lee. "Artificial Neural Networks and their Application to Modelling South African Market Returns", University of Pretoria (South Africa), 2023	<1 %
Publication		

40	kc.sustech.edu.cn	<1 %
Internet Source		

41	sfera.unife.it	<1 %
Internet Source		

42	www.semanticscholar.org	<1 %
Internet Source		

43	zone.biblio.laurentian.ca	<1 %
Internet Source		

Exclude quotes	On
Exclude bibliography	On

Exclude matches	Off
-----------------	-----